

# Modeling grazer-mediated effects of demographic and material connectivity on giant kelp metapopulation dynamics

# A. Raine Detmer\*

Department of Ecology, Evolution, and Marine Biology, University of California, Santa Barbara, CA 93106, USA

ABSTRACT: From dispersal-based metapopulations to meta-ecosystems that arise from flows of non-living materials, spatial connectivity is a major driver of population dynamics. One potentially important process is material transport between populations also linked by individual dispersal. Here, I explored material and demographic connectivity in metapopulations of giant kelp Macrocystis pyrifera, a foundation species that produces both detritus and reproductive spores. Kelp detritus (drift) subsidizes grazers, helping maintain the kelp forest ecosystem state. Drift could potentially be exchanged among kelp patches, but this is less studied than spore dispersal. Therefore, I built an ordinary differential equation (ODE) model to investigate conditions under which drift and/or spore connectivity promotes the kelp forest state. I fit statistical models (generalized linear mixed models, GLMMs) to observational data and used the GLMM's predictions to validate the ODE model. My results suggest kelp patch dynamics are best explained by connectivity of both drift and spores, and that the impacts of these forms of connectivity depend on local grazer (urchin) abundance. Both models predicted greater kelp persistence in well-connected patches across a range of urchin densities. These effects were largely driven by drift, which reduced grazing in recipient patches and thereby enhanced spore recruitment. While testing these predictions will require greater empirical quantification of interpatch drift transport, my findings indicate drift connectivity may be an important spatial process in kelp forest systems. More broadly, this work highlights the role of meta-ecosystem dynamics within a single ecosystem type, reinforcing the need to expand traditional metapopulation perspectives to consider multiple forms of spatial connectivity.

KEY WORDS: Kelp forests  $\cdot$  Meta-ecosystems  $\cdot$  Connectivity  $\cdot$  Mathematical models  $\cdot$  Detritus  $\cdot$  Grazing

- Resale or republication not permitted without written consent of the publisher

## 1. INTRODUCTION

Dispersal of reproductive propagules (e.g. larvae or spores) plays a fundamental role in the population dynamics of many marine species, particularly those with sessile or sedentary adults. Suitable habitat for these species is often patchily distributed, resulting in discrete subpopulations demographically connected by pelagic propagules (Cowen & Sponaugle 2009). Metapopulation theory has proven to be a powerful tool for describing the dynamics of such populations,

providing insight into how dispersal among habitat patches influences persistence and extinction risk (Grimm et al. 2003, Sale et al. 2006, Dedrick et al. 2021). However, a complete understanding of metapopulation dynamics requires consideration of more than demographic connectivity. Spatial heterogeneity in factors affecting patch quality (e.g. resource availability, predation pressure) can lead to variation in rates of recruitment and reproduction, altering local dynamics and patch contribution to the broader metapopulation (Caselle et al. 2003, White & Sam-

houri 2011, Burgess et al. 2014). As marine environments become increasingly impacted by anthropogenic activities, knowledge of the drivers of heterogeneity in patch quality will be essential for the effective management of threatened populations across spatial scales (Gouhier et al. 2013).

Many determinants of local habitat conditions are themselves influenced by spatial processes (Massol et al. 2011, Guichard 2017). For example, a growing body of research has highlighted how the transport of non-living resources (e.g. detrital material, inorganic nutrients) can modify local environments via effects on productivity and trophic interactions (Polis et al. 1997, Loreau et al. 2003, Spiecker et al. 2016). Metaecosystem theory, which combines concepts from metapopulation and metacommunity theory (organismal movement) with landscape ecology (spatial flows of materials), provides a unified framework for describing these dynamics (Loreau et al. 2003, Gounand et al. 2018). In contrast to metapopulations, which typically arise from demographic connectivity among similar habitats, material flows can couple distinct types of ecosystems. Most empirical metaecosystem studies focus on these cross-ecosystem exchanges (Sitters et al. 2015, Peller et al. 2021), such as the well-documented transport of macrophyte wrack from kelp or seagrass beds to beaches (Hyndes et al. 2022). However, theoretical meta-ecosystem models predict that patterns of material flows can alter local dynamics (for example, by creating patches that are nutrient sources or sinks) even without underlying ecosystem heterogeneity (Loreau et al. 2003, Gravel et al. 2010, Marleau et al. 2014). To date, few of these models have been applied to natural systems, resulting in a disconnect between empirical and theoretical meta-ecosystem research and a lack of concrete examples of how metapopulation dynamics may be altered by material flows among their component patches (Gounand et al. 2018, Peller et al. 2021). Here, I began to address this gap by using a combination of mechanistic modeling and statistical analyses to explore the effects of detrital transport within a single marine ecosystem: kelp forests. Specifically, I investigated whether the metapopulation dynamics of a focal species (giant kelp) were influenced by detrital exchange among patches and, if so, how this additional form of connectivity mediated the effects of demographic connectivity on the metapopulation.

Kelp forests are highly productive and diverse ecosystems found on temperate coasts throughout the world. Perhaps the most iconic kelp forests are those formed by the foundation species giant kelp *Macrocystis pyrifera*. Giant kelp strongly regulates the

structure and function of kelp forest communities (Miller et al. 2018, Castorani et al. 2021), and its population dynamics are therefore of both ecological and conservation interest. Like many marine macroalgae, giant kelp produces microscopic spores that are passively transported by currents (Schiel & Foster 2015). Although these spores have short pelagic durations (settling within hours to days of release; Gaylord et al. 2006) and typically travel no more than a few kilometers (Reed et al. 2004, Gaylord et al. 2006), spore dispersal can still be sufficient to connect neighboring reefs (Reed et al. 2006). In southern California, researchers have found relationships between demographic connectivity (spore dispersal) and kelp patch colonization-extinction dynamics, which, together with genetic analyses, suggest that kelp forests in this region function as a metapopulation (Alberto et al. 2010, Castorani et al. 2015, 2017). Connectivity among patches within this metapopulation appears to promote kelp colonization and persistence; however, local factors could potentially influence the magnitude of these effects (Castorani et al. 2015).

One major local driver of kelp dynamics is herbivory. Overgrazing by sea urchins can denude reefs of kelp and inhibit recolonization, resulting in 'urchin barrens' (Ling et al. 2015). Whether reefs exist in kelp forest or barren states can depend on the availability of detrital material, as urchins generally function as cryptic detritivores when detritus (their preferred food source) is plentiful but switch to destructive grazers of living kelp when demand for detritus exceeds supply (Harrold & Reed 1985, Rennick et al. 2022). Most detrital material in kelp forests is drift kelp (hereafter referred to as drift) produced by giant kelp itself (Harrold & Reed 1985) — a consequence of this species' remarkably high productivity and turnover rates (Rassweiler et al. 2018). This introduces the potential for self-reinforcing feedbacks, whereby higher kelp biomass reduces grazing pressure by increasing drift production (Karatayev et al. 2021). Under such conditions, recruitment of externally produced spores could promote kelp persistence in wellconnected patches by increasing kelp population size and thus local drift supply. However, these dynamics assume that locally produced drift is retained within a patch. While rates of drift export from kelp forests are generally poorly quantified, the large inputs of drift observed in adjacent ecosystems (e.g. > 500 kg wet wt  $m^{-1}$  yr<sup>-1</sup> on southern California beaches; Dugan et al. 2011) indicate that export could be fairly high (Krumhansl & Scheibling 2012). If some of this exported drift is transported to other kelp patches, local drift availability could depend not only on local production but

also on input from neighboring patches. Although this has not been explicitly tested in *Macrocystis* forests, a study of *Ecklonia radiata*-dominated reefs in Australia found that urchins were subsidized by drift that was produced on reefs over 2 km away (Vanderklift & Wernberg 2008), suggesting that patch-to-patch exchange of drift is possible and could play a key role in local kelp dynamics.

In this study, I used process-based and statistical models to ask how spore and drift connectivity influence kelp-urchin interactions and kelp metapopulation dynamics in southern California kelp forests. First, I built and analyzed an ordinary differential equation (ODE) model to explore the theoretical conditions under which connectivity of kelp spores and/or drift can promote the kelp forest state. I then validated my model using empirical data collected by the Santa Barbara Coastal Long Term Ecological Research site (SBC LTER) and Channel Islands National Park Kelp Forest Monitoring Program (CINP KFMP) and tested its sensitivity to connectivity parameters to gain insight into the mechanisms underlying observed kelp metapopulation dynamics. The results of these analyses suggest that by increasing the availability of alternative food for urchins, the exchange of drift among kelp patches reduces grazing on new recruits and adult plants and can therefore

play a significant role in local and metapopulationscale kelp forest dynamics.

#### 2. ODE MODEL

## 2.1. Model description

In order to mechanistically explore the effects of kelp spore and drift connectivity on kelp forest ecosystem state, I built an ODE model of giant kelp (meta) population dynamics (Fig. 1). In this section, I describe the main components of this ODE model, starting with the dynamics of a single patch and then introducing a 2-patch system. Details on estimation of model parameters are provided in Table S1 in the Supplement at www.int-res.com/articles/suppl/m726p049\_supp.pdf.

## 2.1.1. Giant kelp stage structure

Giant kelp has a heteromorphic life cycle. A microscopic haploid gametophyte generation alternates with canopy-forming diploid sporophytes, each of which consists of rope-like buoyant fronds attached to the sea floor by a single holdfast. Following Detmer

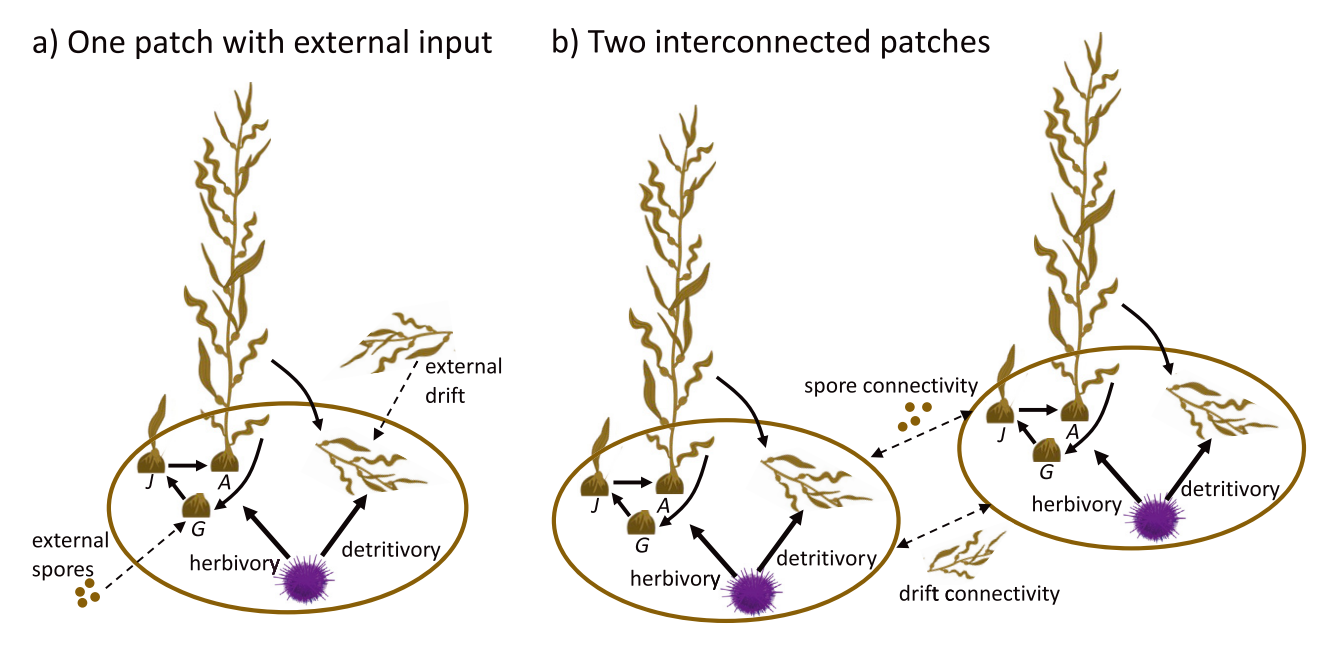


Fig. 1. Conceptual diagram of the ordinary differential equation (ODE) model. Adult sporophytes (A) produce spores that develop into gametophytes (G), which in turn produce juvenile sporophytes (J) that mature into the next generation of adult sporophytes. Urchins consume drift (either locally produced or imported) but begin to graze all kelp life stages if drift supply is limited. (a) Single-patch model with constant external supply of spores and/or drift. (b) Two-patch model with exchange of spores and drift between patches. Image credits: Jane Thomas (giant kelp), Tracey Saxby (sea urchin); Integration and Application Network, University of Maryland Center for Environmental Science (https://ian.umces.edu/imagelibrary/)

et al. (2021), I accounted for this complex life cycle by including 3 life stages in my model: gametophytes, juvenile sporophytes (defined as sporophytes with fronds < 1 m tall), and adult sporophytes.

Gametophytes,  $G_i$  arise from externally and locally produced spores. External spores enter the patch at a rate  $\varepsilon_s$  (see Table 1 for all ODE model parameters and their values). Spores are also produced locally by adult sporophytes at a per-biomass rate  $\rho$  (Neushul 1963). I calculated total patch biomass (kg adult kelp  $m^{-2}$ ) as the product of biomass per kelp individual, b (representing average individual biomass across adults in the patch) and the density of adult sporophytes, A (ind. m<sup>-2</sup>). Thus, the total rate of local spore production is given by  $\rho bA$ . A fraction  $l_s$  of these spores are transported out of the patch, while the remaining fraction  $(1 - l_s)$  are retained. Gametophytes recruit to the sporophyte stage at a per capita rate  $r_G$ and experience background mortality at a densitydependent rate  $\mu_G$  (Reed 1990), meaning their per capita background mortality rate is  $\mu_G G$ . Finally, they experience mortality from sea urchin herbivory at a per capita rate  $H_G$  (described in Section 2.1.2 below). The change in gametophyte density over time is therefore given by:

$$\frac{\mathrm{d}G}{\mathrm{d}t} = \varepsilon_s + (1 - l_s)\rho bA - r_G G - H_G G - \mu_G G^2 \quad (1)$$

Juvenile sporophytes, J, arise from the recruitment of gametophytes ( $r_GG$ ). Given that my model tracks densities of individuals, and it takes one male and one female gametophyte to produce a single sporophyte, I multiplied this rate by 0.5 (male and female gametophytes appear to occur in equal ratios; Reed 1990). Juvenile sporophytes mature into adults at a rate  $r_J$ . They experience background mortality at a density-dependent rate  $\mu_J$  and urchin herbivory at a rate  $H_J$ :

$$\frac{\mathrm{d}J}{\mathrm{d}t} = 0.5r_G G - r_J J - H_J J - \mu_J J^2$$
 (2)

The density of adult sporophytes, A, increases at a rate dependent on juvenile maturation as well as the availability of limiting resources (e.g. benthic space and light; Graham et al. 1997) in the patch. The maximum adult density the patch can support is given by the carrying capacity K. Adults experience background mortality at a rate  $\mu_A$  and urchin herbivory at a rate  $H_A$ . The change in adult density over time is thus described by:

$$\frac{\mathrm{d}A}{\mathrm{d}t} = r_J J \left( 1 - \frac{A}{K} \right) - H_A A - \mu_A A \tag{3}$$

In this formulation, density-dependent mortality occurs during the transition from the juvenile to adult

sporophyte stage (e.g. if adults are at carrying capacity, maturing juveniles die due to lack of space, light, or other resources), and additional adult background mortality—such as death at end of lifespan—is assumed to be density-independent. For all life stages, mortality from disturbance was modeled by reducing initial densities (see Section 2.2).

Adult sporophytes produce drift (e.g. senesced blades and fronds) at a per-biomass rate, d. This rate is multiplied by patch biomass density bA to obtain the total rate of drift production (I assumed that drift production by juvenile sporophytes is negligible). Similar to spores, a fraction  $l_d$  of this drift is exported from the patch, while a fraction  $(1-l_d)$  is retained. Externally produced drift kelp enters the patch at a rate  $\epsilon_d$ . Thus, the rate of drift supply from external and local sources can be expressed as:

$$\varepsilon_d + (1 - l_d) \mathrm{d}bA \tag{4}$$

#### 2.1.2. Urchin grazing

In my model, sea urchin density (u) is assumed constant, as urchin populations typically fluctuate over longer time scales than kelp and exhibit sporadic recruitment dynamics dependent on large-scale climatic conditions (Shears et al. 2012, Okamoto et al. 2020). I allowed urchins to feed on both drift (detritivory) and live kelp (herbivory). I assumed that urchins consume drift at a constant per capita rate  $g_d$ ; thus, the total rate of drift consumption is  $q_d u$ . Urchins consume living adult sporophytes, juvenile sporophytes, and gametophytes at maximum per capita rates g,  $q_Iq_I$  and  $q_Gq_I$  respectively; the coefficients  $q_I$  and  $q_G$ scale the maximum grazing rates on juvenile sporophytes and gametophytes relative to that of adults, with values greater than one accounting for the higher vulnerability of early life stages to herbivory (Dayton et al. 1984).

There is strong evidence that urchins preferentially consume drift but begin to actively graze live kelp when drift supply becomes limited (Harrold & Reed 1985, Rennick et al. 2022). This behavioral switch has previously been modeled using a Type IV functional response (Koen-Alonso 2007) in which the per capita rate of urchin herbivory declines with increasing drift availability (Karatayev et al. 2021). Recent work suggests that the ratio of drift production to urchin drift consumption (rather than the absolute amount of drift per se) is a strong determinant of grazing pressure on living kelp (Rennick et al. 2022). I therefore modeled urchin behavior (i.e. the pro-

portional change in herbivory rate relative to the maximum rate, g) using a function B(u,A), which incorporates this ratio into a modified Type IV functional response (Eq. 5; note that unlike Karatayev et al. 2021 and Rennick et al. 2022, which focused on the scale of individual reefs, here I consider both local and external drift production). When there are no urchins, B(u,A) = 0. For urchin densities >0, B(u,A) depends on the ratio of rates of drift production and consumption, as well as a scaling factor p that controls how rapidly urchins switch to detritivory with increasing drift availability (Fig. S1).

$$B(u,A) = \begin{cases} 0, & u = 0\\ \frac{1}{1 + \frac{1 - p}{p} \left(\frac{\text{drift production}}{\text{drift consumption}}\right)^{2}}, & u > 0 \end{cases}$$

$$= \begin{cases} 0, & u = 0\\ \frac{1}{1 + \frac{1 - p}{p} \left(\frac{\varepsilon_{d} + (1 - l_{d})dbA}{g_{d}u}\right)^{2}}, & u > 0 \end{cases}$$

$$(5)$$

Rates of urchin herbivory on each kelp life stage are calculated as the products of the maximum rates of herbivory and the value of behavioral function B(u,A):

$$H_G = q_G q u B(u_t A) \tag{6}$$

$$H_{I} = q_{I}quB(u_{I}A) \tag{7}$$

$$H_A = guB(u,A) \tag{8}$$

When urchins are present and there is no drift production, B(u,A) = 1 and herbivory occurs at its maximum rate. As the ratio of drift production to consumption increases, urchins are increasingly satisfied by feeding on drift, and B(u,A) (and thus herbivory) declines towards zero.

# 2.1.3. Two patches and patch connectivity

To extend my model to 2 patches, I kept local dynamics the same but altered the external input terms to allow for connectivity between patches (Fig. 1b). The fractions of spores and drift that leave patch i and successfully disperse to patch j are given by the connectivity parameters  $c_s$  (for spores) and  $c_d$  (for drift). Both  $c_s$  and  $c_d$  range from 0 (no connectivity between patches) to 1 (everything that leaves one patch goes to the other). I assumed that imported spores and drift are evenly distributed in the recipient patch and that both patches have the same area, so rates of spores and drift settlement are equal to the product of production rates in the source patch (which are per  $m^2$ ; Table 1) and the fraction of this production trans-

ported to the recipient patch. Thus, import rates in patch i are calculated as  $c_s l_s \rho b A_j$  for spores and  $c_d l_d db A_j$  for drift. The full equations for patch i in the 2-patch model are shown in Eqs. (9) to (12).

$$\frac{dG_{i}}{dt} = c_{s}l_{s}\rho bA_{j} + (1 - l_{s})\rho bA_{i} - r_{G}G_{i} - q_{G}guB(u, A_{i}, A_{j})G_{i} - \mu_{G}G_{i}^{2}$$
(9)

$$\frac{\mathrm{d}J_{i}}{\mathrm{d}t} = 0.5r_{G}G_{i} - r_{J}J_{i} - q_{J}guB(u, A_{i}, A_{j})J_{i} - \mu_{J}J_{i}^{2}$$
 (10)

$$\frac{\mathrm{d}A_i}{\mathrm{d}t} = r_J J_i \left( 1 - \frac{A_i}{K} \right) - guB(u, A_i, A_j) A_i - \mu_A A_i \tag{11}$$

$$B(u, A_i, A_j) = \begin{cases} 0, & u = 0\\ \frac{1}{1} & u > 0\\ 1 + \frac{1 - p}{p} \left( \frac{c_d l_d db A_j + (1 - l_d) db A_i}{g_d u} \right)^2, & u > 0 \end{cases}$$
(12)

# 2.2. Model analyses and results

To investigate the effects of spore and drift connectivity on kelp forest-urchin barren dynamics, I first used the single patch version of the ODE model to evaluate how external spores and drift influence the system's stability. Here and throughout the study, I simulated scenarios in which there was external input/connectivity of (1) spores only, (2) drift only, and (3) spores and drift together. This allowed me to distinguish the effects of spores versus drift on system dynamics and to bracket a range of possible connectivity scenarios, from fully decoupled (spores or drift only) to fully coupled (spores and drift). I calculated the equilibrium abundance of adult kelp as a function of urchin density and external supply of spores and/or drift. Rates of external input ranged from minima of zero to maxima equal to the equilibrium export rates of an isolated, urchin-free source patch (i.e.  $l_s \rho b A_{\text{source}}^{\star}$  for spores and  $l_d db A_{\text{source}}^{\star}$  for drift, where  $A_{\text{source}}^{\star}$  is the equilibrium adult sporophyte density in the source patch). Thus, these simulations can be thought of as an island-mainland scenario in which varying fractions of spores and drift produced in a fixed 'mainland' patch disperse to a dynamic 'island' patch.

The model exhibits a region of bistability in which both high and low kelp population states can exist at the same density of urchins (Fig. 2). If kelp density is initially high, the system equilibrates at the high kelp state because urchins are satisfied by drift supply; however, if kelp density is initially low or declines, starving urchins exert strong grazing pressure that keeps the kelp population in the low (barren) state.

Table 1. Ordinary differential equation (ODE) model state variables and parameters. Details on estimation of parameter values are provided in Table S1

	Units	Default value
hytes	ind. $m^{-2}$	_
sporophytes	ind. $m^{-2}$	_
prophytes	ind. $m^{-2}$	_
- •	Days	_
	$d^{-1}$	0.05
	$G^{-1}$ $\mathrm{d}^{-1}$	0.6
on rate	$d^{-1}$	0.004
rate	$J^{-1} \ { m d}^{-1}$	0.01
pacity	ind. $m^{-2}$	1
te	$\mathrm{d}^{-1}$	0.002
	kg ind. <sup>–1</sup>	7
ction rate	spores $kg^{-1} d^{-1}$	10
tion rate	$kg drift kg^{-1} d^{-1}$	0.024
	ind. $m^{-2}$	Varied
rchins	$kg drift u^{-1} d^{-1}$	0.0011
prophytes	ind. $u^{-1} d^{-1}$	0.025
tophytes relative to adults	_	1.2
ile sporophytes relative to adults	_	1.2
to max.) if rates of drift production	_	0.1
	$\rm spores\ m^{-2}\ d^{-1}$	Varied
	$kg drift m^{-2} d^{-1}$	Varied
res that leave patch	_	0.5
t that leaves patch	_	0.5
	_	Varied
ransported to patch $j^{\mathrm{b}}$	_	Varied
1	$i$ transported to patch $j^{\rm b}$ ransported to patch $j^{\rm b}$	i transported to patch j <sup>b</sup> –

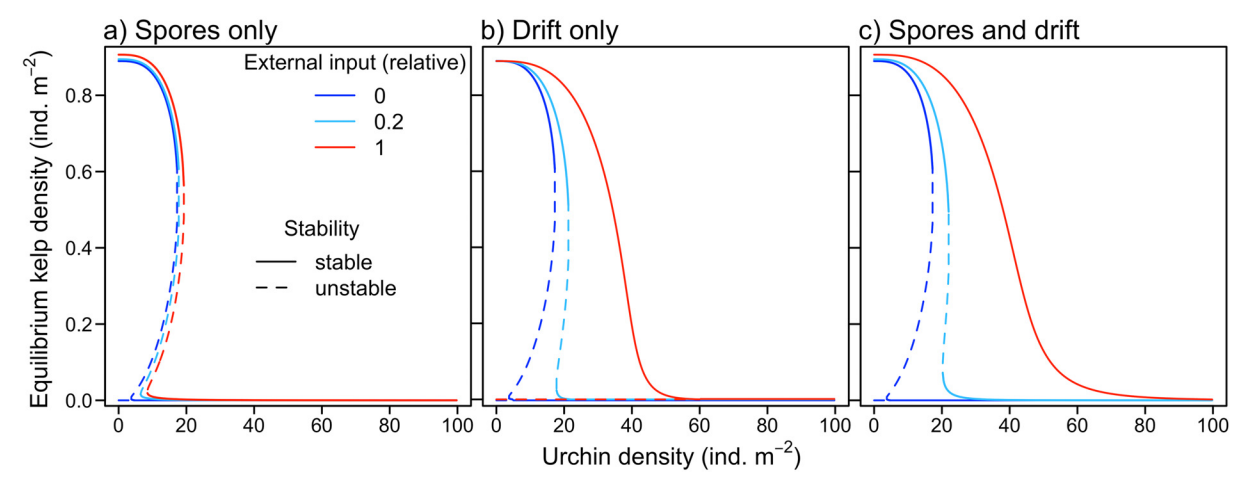


Fig. 2. Effect of urchins and external input of spores and drift kelp on equilibrium kelp density. The *x*-axis is the density of urchins (*u*) and the *y*-axis is the equilibrium density of adult kelp sporophytes ( $A^*$ ). Solid and dashed lines indicate stable and unstable equilibria, respectively. Line color represents external supply rate of (a) spores ( $\varepsilon_s$ ), (b) drift ( $\varepsilon_d$ ), or (c) both spores and drift. External inputs are expressed as a fraction, *f*, of export rates from an isolated urchin-free source patch at equilibrium; i.e.  $\varepsilon_s = fl_s pbA^*_{\text{source}}$  and  $\varepsilon_d = fl_d dbA^*_{\text{source}}$ , where *f* is equal to 0 (dark blue), 0.2 (light blue), or 1 (red). In (a), there is no input of drift ( $\varepsilon_d = 0$  in all cases), and in (b) there is no spore input ( $\varepsilon_s = 0$ ). Equilibria and their stability were calculated using Mathematica v13.0

External input of either spores or drift decreases the bistable region and shifts it to higher urchin densities, but this effect is smaller for spores (Fig. 2a) than for drift (Fig. 2b). High enough levels of drift input cause the region of bistability to disappear, and kelp state depends only on urchin density. Although drift input expands the region where only non-zero kelp densities are stable, drift alone does not enable an initially barren patch to recover  $(A^* = 0)$  is always an unstable equilibrium in Fig. 2b) because external spores are needed for kelp to recolonize. These more subtle effects of spores are apparent when there is external input of both spores and drift (Fig. 2c). While the system's dynamics are generally similar to the drift-only case, the high kelp state stabilizes at higher kelp densities and there is no longer an unstable zerokelp equilibrium.

The range of urchin densities over which the system exhibits bistability is also sensitive to local parameters (Figs. S2 & S3). For instance, increasing biomass per kelp plant (b) allows kelp to persist at higher urchin densities due to greater local drift and spore production, while reducing drift retention ( $l_d$ ) (e.g. representing patches with low substrate complexity; Randell et al. 2022) causes the barren state to be stable at lower urchin densities (Fig. S2). However, regardless of local conditions, external drift always had a larger effect on kelp stability than external spore input (Fig. S3).

Having considered a constant external supply of spores and drift in the 1-patch model, I next used the 2-patch model (Fig. 1b) to study the effects of feedbacks between metapopulation dynamics and the supply of spores and drift. I first explored how the level and type of connectivity influence kelp recovery from disturbance events (e.g. winter storms; Reed et al. 2011) across a range of urchin densities. Here, connectivity is represented as the fractions of spores  $(c_s)$ and drift  $(c_d)$  transported out of one patch that enter the other. For simplicity, I assumed  $c_s$  and  $c_d$  were the same for both patches (connectivity is symmetric) and that the fractions of spores and drift leaving a patch ( $l_s$ and  $l_d$ , respectively) were the same for both patches. Such a scenario is unlikely to apply to natural reefs; however, it is useful for developing a basic theoretical understanding of this model's dynamics. I again considered spore only ( $c_d = 0$ ,  $0 \le c_s \le 1$ ), drift only ( $c_s =$  $0, 0 \le c_d \le 1$ ), and both spore and drift ( $0 \le c_s \le 1$ ,  $c_d =$  $c_s$ ) connectivity scenarios. Both patches were given identical parameters, and I focused on the dynamics of Patch 1 (hereafter referred to as the focal patch).

For each combination of connectivity values and urchin densities, I determined whether (1) only the

high kelp state was stable (kelp recovers even if starting from low initial conditions; i.e.  $A_0 = 0$ ), (2) only the barren state was stable (kelp goes to the barren state even if starting at high initial conditions; i.e.  $A_0 = A_{0high}$ ), or (3) the system was bistable. When the system was bistable, I calculated the lowest initial kelp density (representing kelp density immediately following a disturbance) that the focal patch could tolerate before it failed to recover to the high state within 2000 d. The 2000 d cutoff was chosen both to reduce computational time and because longer recovery times are less relevant for kelp forests, where disturbance frequency is generally <5 yr (1825 d; Byrnes et al. 2011). For each value of  $A_0$  tested, I calculated the corresponding initial densities of G and J as a function of disturbance severity (measured as  $A_0 / A_{0high}$ , the proportional reduction in adult density if the patch had been at the high kelp equilibrium pre-disturbance). I assumed these early life stages were also disturbed, but to a lesser degree than adult sporophytes (see Table S2 for initial conditions used). I repeated these analyses for local disturbances (affecting only the focal patch; non-focal patch starts at high initial conditions) and regional disturbances (affecting both patches equally; both patches have the same initial conditions). I recorded the state of both patches at the end of each simulation. All simulations here and in the rest of the study were performed using deSolve (v1.31; Soetaert et al. 2010) in R (v4.0.5; R Core Team 2021).

The effect of connectivity on kelp recovery from disturbance depended on both the type of connectivity and the scale of the disturbance event (Fig. 3). Exchange of drift (and, to a lesser extent, spores) between patches increased the maximum urchin density for which kelp could exist in the high state (upper black lines in Fig. 3). Below this maximum urchin density, connectivity - especially of drift - allowed kelp to withstand greater levels of disturbance without tipping to the barren state; however, the magnitude of this effect differed between local and regional disturbances. For regional disturbances, higher connectivity was effectively the same as greater selfretention, as the 2 patches were identical. Consequently, connectivity could not promote recovery from disturbances that fully removed kelp from the system. When disturbances were localized, the undisturbed patch remained a source of spores and/or drift. Connectivity therefore expanded the range of urchin densities for which kelp recovery was always possible, with drift again having a larger effect than spores (Fig. 3a-c).

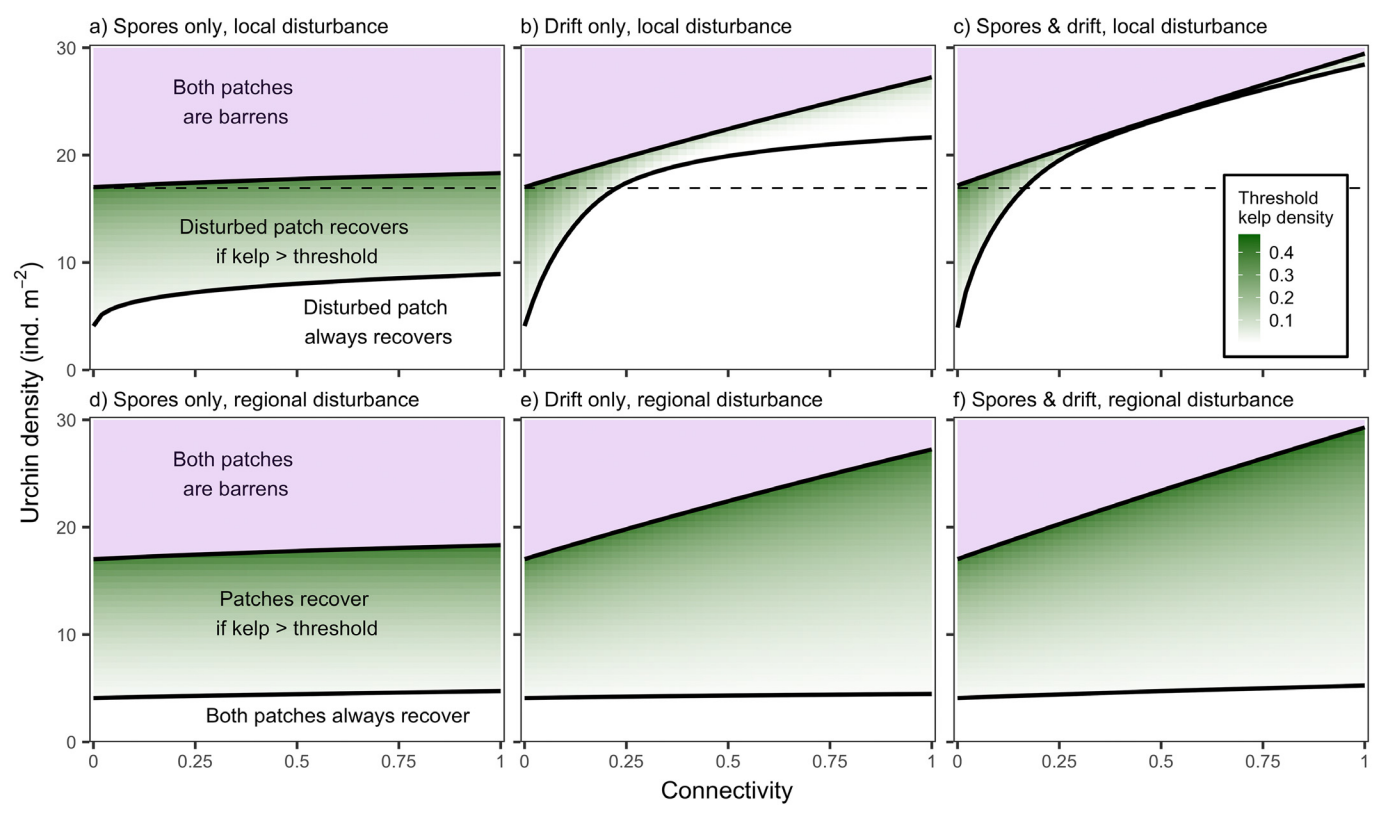


Fig. 3. Impacts of disturbance on 2 kelp patches with varying levels of connectivity and urchin densities. Connectivity is either of spores only ( $c_s$ , left column), drift only ( $c_d$ , middle column), or both ( $c_s = c_d$ , right column). Purple denotes regions where both patches are always in the barren (low kelp) state. Black solid lines border the range of urchin densities for which the focal patch is bistable; within this region, green shading indicates the maximum disturbance severity (= minimum adult kelp density; referred to as the threshold kelp density in the figure) the focal patch can withstand and still recover to the high kelp state. In (a–c), disturbances are local (impact only the focal patch), while in (d–f) they are regional (both patches equally disturbed). The dashed line in (a–c) shows the upper boundary of the region of bistability for an isolated patch (i.e. when  $c_d = c_s = 0$ ). Where the region of bistability of the coupled 2-patch system extends above this line, collapse of the kelp population in the focal patch causes the undisturbed patch to also flip to the barren state, while below this line the undisturbed patch remains in the high kelp state

Local disturbances produced more complex interpatch dynamics than regional disturbances. When the system was bistable, a disturbance that tipped the focal patch into the barren state could also cause the undisturbed neighboring patch to collapse due to a reduction in spore and/or drift supply (Fig. S4a). For the case with only spore connectivity, these dynamics occurred at all urchin densities between the upper boundaries of the bistable region in the absence and presence of connectivity (dashed and upper solid black lines in Fig. 3a). For cases with drift connectivity (Fig. 3b,c), an additional scenario emerged in which the region where only the high kelp state was stable extended past the upper bistability boundary of an isolated patch. Here, initially high drift input from the undisturbed patch ensured that the recovery of the disturbed patch was rapid enough for the undisturbed patch to persist, and both were able to return to the high kelp state (Fig. S4b).

In kelp forests, many disturbance events (e.g. storms, marine heatwaves) occur over spatial scales larger than the distances between connected kelp patches. Such events are better represented in my model as regional disturbances (Fig. 3d-f). I therefore explored the system's ability to recover from regional disturbance in greater detail by investigating how spatial variation in urchin density (e.g. due to differences in recruitment; Okamoto et al. 2020) altered the effects of connectivity on patch recovery. I ran simulations with various combinations of urchin densities in Patch 1 and Patch 2 and, for each combination, calculated the stability of high kelp and barren states in each patch (indicating recovery potential; see above). I repeated this process with no connectivity between the patches and with high connectivity of spores and/or drift.

When patches were interconnected, reducing the density of urchins in one patch relative to the other could benefit kelp populations in both patches (expan-

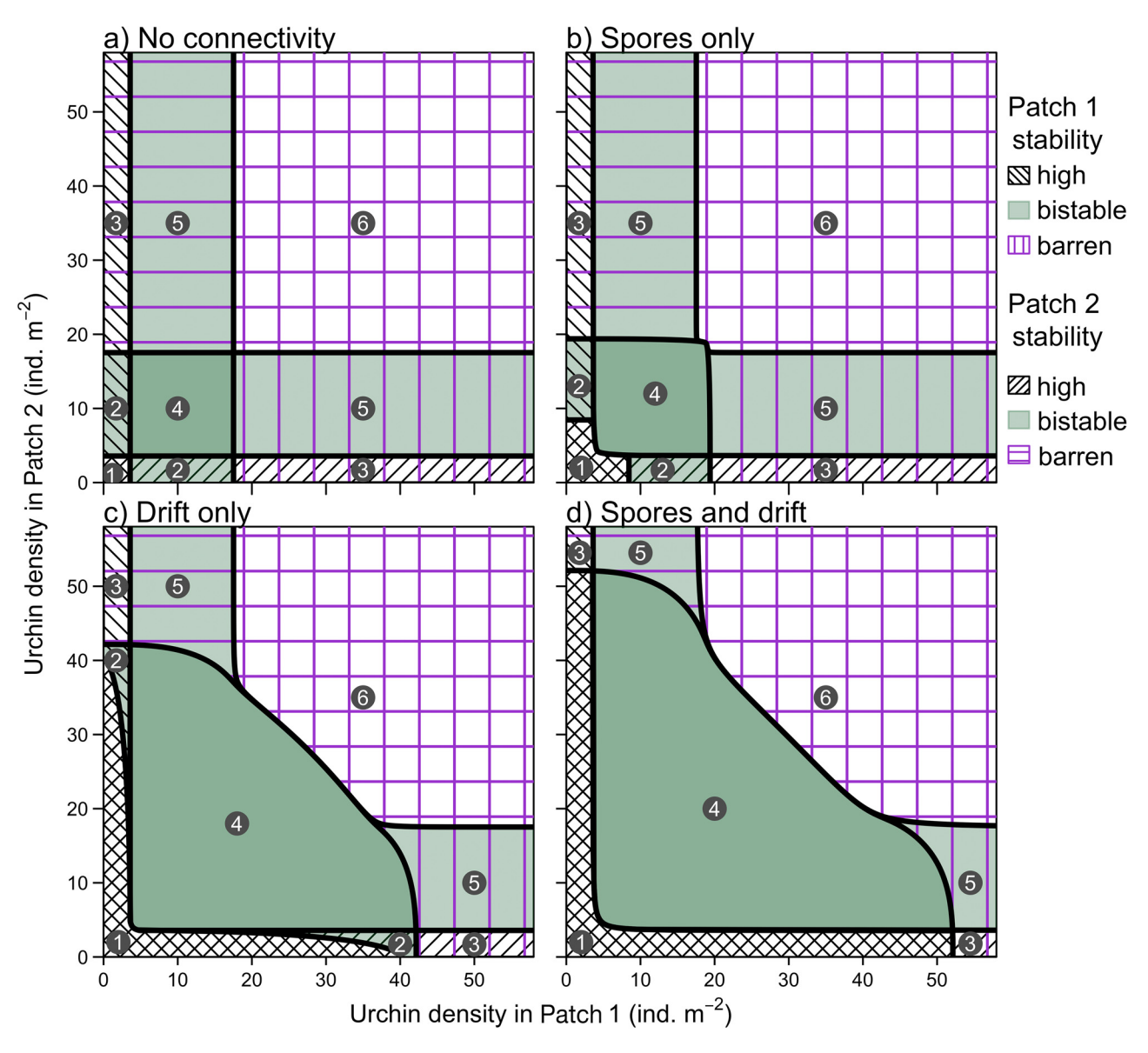


Fig. 4. Effect of connectivity between patches with different urchin densities on kelp stability (and thus recovery potential). The x- and y-axes are the densities of urchins in Patch 1 and Patch 2, respectively. Regions of patch stability are labeled as follows: (1) only the high kelp state is stable in both patches, (2) only the high kelp state is stable in one patch and the other patch is bistable, (3) only the high kelp state is stable in one patch and only the barren (low kelp) state is stable in the other, (4) both patches are bistable, (5) one patch is bistable and only the barren state is stable in the other, and (6) only the barren state is stable in both patches. (a) No connectivity between the patches ( $c_s = c_d = 0$ ), (b) high spore connectivity only ( $c_s = 1$ ,  $c_d = 0$ ), (c) high drift connectivity only ( $c_s = 0$ ,  $c_d = 1$ ), and (d) high connectivity of both spores and drift ( $c_s = c_d = 1$ )

sion of regions 1 and 4 in Fig. 4b—d relative to Fig. 4a). For example, if urchin densities were near zero in Patch 1, connectivity increased the range of urchin densities for which Patch 2 could recover from disturbance because the stable kelp population in Patch 1 served as a source of spores or drift for Patch 2. Similarly, when urchin densities in Patch 1 were within the range for which this patch was bistable in the absence of connectivity, adding connectivity in-

creased the range of urchin densities for which Patch 2 was bistable rather than always barren. Connectivity also enabled both patches to be bistable at combinations of urchin densities that would have caused them to be barren if in isolation (replacement of part of region 6 with region 4 in Fig. 4). Recall that bistability means that kelp can recover only if disturbances are not severe enough to tip the patch into the barren state; thus, for regions in which one or both patches

are bistable, kelp could exist in either high or low (barren) states depending on past disturbance regimes. The effects of connectivity described above were stronger for drift than spores (Fig. 4b vs. 4c) but had the greatest impact when there was connectivity of both (Fig. 4d).

## 3. EMPIRICAL ANALYSES

The results of the above analyses provide mechanistic insight into how different forms of connectivity may influence kelp forest dynamics. I next asked whether my ODE model's theoretical predictions were consistent with published data from southern California kelp forests. In the following sections, I briefly introduce these data, describe my statistical analyses, and use the statistical results to validate my ODE model and address uncertainty in connectivity parameters.

## 3.1. Empirical data

The goal of my empirical analyses was to explore how observed local (within-patch) relationships between urchins and giant kelp are influenced by connectivity among kelp forest patches. At the local scale, the SBC LTER site and CINP KFMP provide annual estimates of giant kelp and sea urchin densities in permanent transects in and around the Santa Barbara Channel (Fig. S7). I used transect-level urchin densities (summed across the 2 most common species, Strongylocentrotus purpuratus and Mesocentrotus franciscanus, and averaged across quadrats within each transect) as my measure of within-patch urchin abundance. For giant kelp, I classified a transect as being in either a high kelp state (>0.05 ind. m<sup>-2</sup>) or a low kelp state, as this binary categorization is better aligned with my ODE model predictions than continuous densities. The threshold density of 0.05 ind. m<sup>-2</sup> represents the 15th density quantile of observations with kelp and has previously been used as the cut-off for a kelp-dominated state in the Channel Islands (Karatayev et al. 2021). More details on these data are given in Section 3 of the Supplement. For full descriptions, see Kushner et al. (2013) and SBC LTER et al. (2022a,b).

For metrics of connectivity, I used giant kelp metapopulation data published by Castorani et al. (2017). These data include the location and area of every kelp patch in southern California (as identified by Cavanaugh et al. 2014; Fig. 5a), as well as satellite-derived estimates of kelp canopy biomass in each patch (Cavanaugh et al. 2019, Castorani et al. 2022b). The authors also used Regional Oceanic Modeling System (ROMS) solutions for the Southern California Bight to estimate average dispersal times of Lagrangian particles between all pairs of patches (Castorani et al. 2022c; see Castorani et al. 2015, 2017 and Section 3 of the Supplement for more details). Both patch biomass and dispersal times were averaged over each semester (Jan-Jun and Jul-Dec) between 1996 and 2006. To convert interpatch dispersal times into measures of propagule connectivity, I followed the approach used in Castorani et al. (2015). Briefly, I assumed that propagules are lost (e.g. due to mortality or settlement en route) at a constant daily proportional rate,  $\lambda$ . For any semester S with an average dispersal time of  $t_{ij,S}$  days, the probability of successful dispersal from patch i to j is given by:

$$P_{ii,S} = (1 - \lambda)^{t_{ij,S}} \tag{13}$$

These dispersal times account for asymmetry in currents; in general,  $t_{ij} \neq t_{ji}$ . I chose a default value of  $\lambda = 0.9 \, \mathrm{d^{-1}}$  (Castorani et al. 2015) but also calculated connectivity for a range of  $\lambda$  values to evaluate the sensitivity of my statistical analyses to this parameter. I note the ROMS dispersal times used here may be more representative of spore dispersal than transport of drift kelp. Much less is known about the latter, which I address in a later section.

Eq. (13) provides an estimate of potential connectivity between a source and destination patch. Total realized patch connectivity (i.e. the amount of propagules or material arriving in the destination patch) is also dependent on production in each source patch. Production of spores and drift are proportional to kelp biomass (Neushul 1963, Schiel & Foster 2015, Rennick et al. 2022); thus, realized connectivity from patch i to j in semester S can be approximated as the product of the average canopy biomass in patch i,  $b_{Ci,Si}$ , and the potential connectivity,  $P_{ij,Si}$ . Total realized connectivity (hereafter referred to as patch connectivity) of a patch j in semester S is given by the sum of its realized connectivities with each source patch  $i \neq j$ :

patch connectivity 
$$_{j,S} = \sum_{i \neq j}^{n} b_{Ci,S} (1 - \lambda)^{t_{ij,S}}$$
 (14)

where n is the total number of patches in the metapopulation.

The metapopulation data cover a greater spatial extent and narrower time period than the benthic monitoring data. To integrate these datasets, I selected patches containing transects and the transects within these patches. For each patch—transect combination,

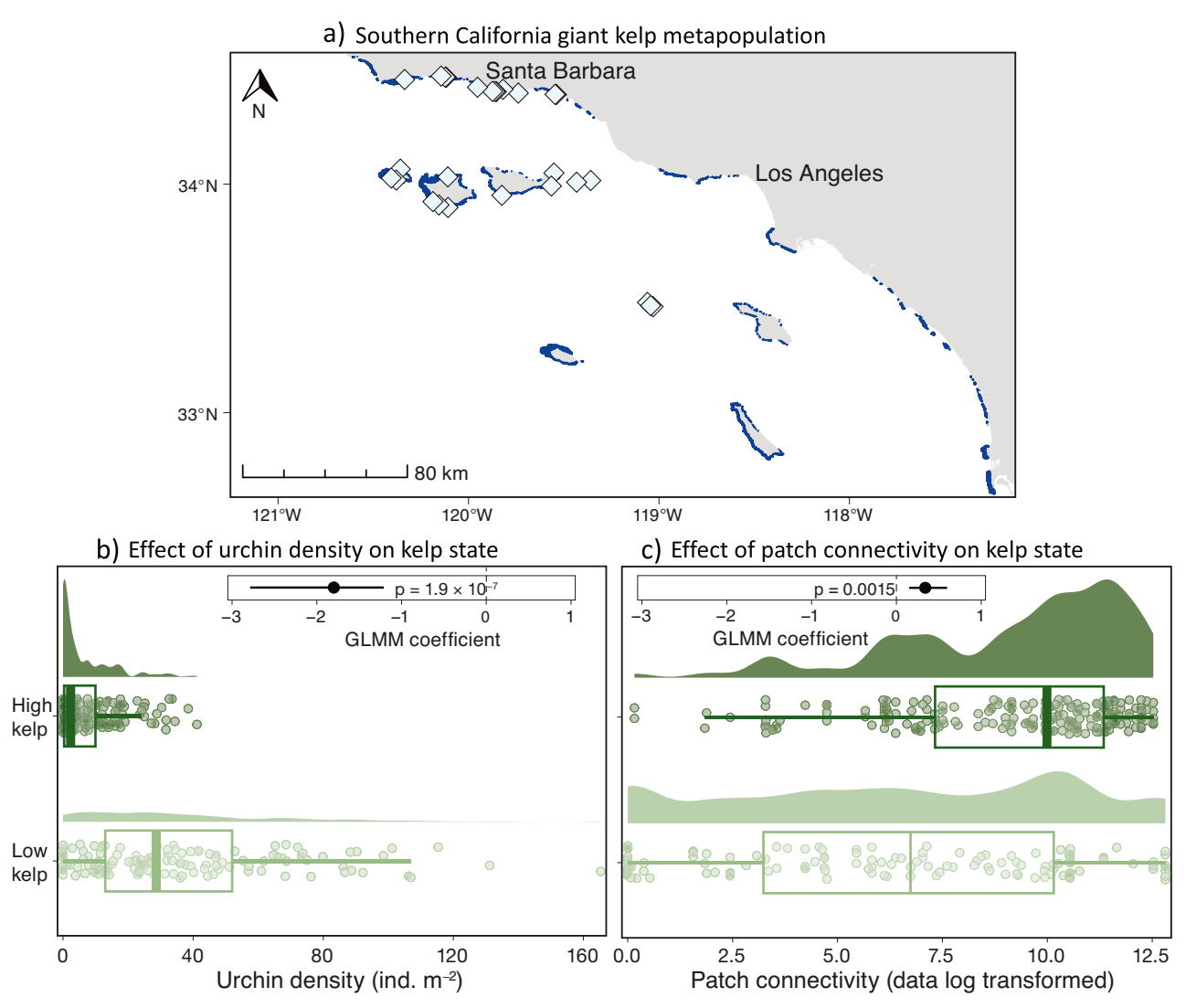


Fig. 5. (a) Study region, with dark blue regions indicating locations of giant kelp metapopulation patches. Focal patches containing benthic transect data on kelp and urchin densities are marked with light blue diamonds. (b) Urchin densities in focal transects in the high (>0.05 ind.  $m^{-2}$ ) and low ( $\leq$ 0.05 ind.  $m^{-2}$ ) kelp states; note these values were log transformed for the generalized linear mixed effects model (GLMM) fitting but are shown here on the raw scale. Each point corresponds to an observation in a transect in a single year. (c) Patch connectivity (log + 1 transformed) of the patches containing focal transects in the high and low kelp states. The boxplots in (b) and (c) show the 25th, 50th, and 75th percentiles of the data, with the whiskers extending 1.5× the length of the inter-quartile range past the box edges (or to the end of the range of the data, if that comes first). The insets in (b) and (c) show the estimated coefficients, bootstrapped 95% confidence intervals, and associated p-values for the effects of urchin density and patch connectivity on the high kelp state in the fitted GLMM described in the main text

I only used data from years for which there were both urchin abundance data and kelp connectivity estimates. To produce a single set of observations for each year, I used values of patch connectivity from the semester prior to each annual survey date (repeating the statistical analyses below with shorter and longer lags in connectivity confirmed this one-semester lag was most predictive). The resulting data set contained 25 patches, 52 transects (1–8 transects patch<sup>-1</sup>), and 2–11 yr of data for each patch—transect combination (Fig. 5).

## 3.2. Statistical analyses and results

I used the empirical data described above to ask whether metapopulation characteristics and urchin abundance influence the probability of a transect being in the high kelp state. The data have a nested structure (transects within patches), repeated measures (multiple observations at each location), and a binary response variable (kelp state). I therefore addressed my question using a binomial GLMM with a logit link function. I included patch connectivity,

patch area (which has been shown to play a significant role in giant kelp patch dynamics; Castorani et al. 2015, 2017), and transect-level urchin density as fixed effects. Transect and year were used as random intercept effects. Patch was not included as a random effect because it had near-zero variance that caused convergence and singularity issues; removing it improved fitting and had no effect on model results. I specified *a priori* a series of GLMMs with all combinations of my 3 fixed effects as well as an explicit urchin density—patch connectivity interaction (Table S3). The full model is given by:

kelp\_state<sub>ijk</sub> ~ Binominal(1, 
$$p_{ijk}$$
)

logit( $p_{ijk}$ ) = urchin\_density<sub>ij</sub>

+ patch\_connectivity<sub>jk</sub> + urchin\_density<sub>ij</sub>

× patch\_connectivity<sub>jk</sub> + patch\_area<sub>k</sub> (15)

+ transect<sub>i</sub> + year<sub>j</sub> transect<sub>i</sub> ~N(0,  $\sigma^2_{\text{transect}}$ )

year<sub>j</sub> ~N(0,  $\sigma^2_{\text{year}}$ )

where kelp\_state $_{ijk}$  is the state of the kelp population (high or low) in transect i, patch k, and year j, and all fixed effects are log or (log +1) transformed to improve model fitting. Fitting was done using the 'lme4' package (v1.1.28; Bates et al. 2015) with maximum likelihood estimation by the Laplace approximation (Bolker et al. 2009). After fitting, I assessed model parsimony using Akaike's information criterion (AIC) and  $\Delta$ AIC values, checked that the best-fitting model met GLMM assumptions (no multicollinearity, independence and lack of patterns in residuals, normally distributed random effects; Zuur et al. 2009), and evaluated the significance of fixed effects using the Wald  $\chi^2$  test.

The most parsimonious model contained urchin density, patch connectivity, and patch area as independent fixed effects, all of which were significant (p =  $6 \times 10^{-8}$ , 0.0013, and 0.02, respectively; Table S3, Fig. S15). The effect of urchin density on the high kelp state was negative (Fig. S15). Patch connectivity and patch area both had positive effects (Fig. S15), consistent with previous studies of this metapopulation (Castorani et al. 2015, 2017). This model generally conformed well to assumptions (Figs. S9–S11), although the residuals showed several outliers (4 of 349 data points). Some of these were likely due to high sand cover (Figs. S13 & S14), while the others were possibly due to interannual kelp cohort dynamics (Fig. S14). Re-fitting the models without these outliers improved residuals (Fig. S12) and generally had minimal effects on model selection and final output (the most parsimonious model remained the same, with  $p=2\times 10^{-7}$ , 0.0015, and 0.02 for effects of urchins, connectivity, and area, respectively; Table S3, Figs. S15–S17, Fig. 5). I therefore used the model fitted without outliers for further analyses, but report results for both versions in the supplement. Model selection and predictions were robust to the value of the loss rate ( $\lambda$ ) used to calculate patch connectivity (Fig. S18) as well as the threshold kelp density for the high kelp state (Fig. S19).

I used the best-fitting GLMM to predict the probability of kelp being in the high state as a function of urchin density and patch connectivity. I repeated this across a set of urchin densities between 0 and 50 urchins  $\rm m^{-2}$  (a range that captures 90% of observed densities in the dataset) and the 10 and 90% quantiles of patch connectivity (representing patches with low and high connectivity, respectively). Patch area was set to its mean value, and the random effects of transect and year were set to zero.

#### 4. MODEL VALIDATION

In this section, I parameterized my single-patch ODE model (Eqs. 1–8) for the study region, used it to generate probabilities of observing kelp in the high state, and compared these predictions to those of the GLMM model described above. These analyses served 2 purposes. First, they enabled me to validate the ODE model by demonstrating that it could produce predictions similar to those of the GLMM. Second, by repeating the ODE simulations for different types of kelp connectivity (spores, drift, or both) and seeing which scenario most closely matched the GLMM's predictions, I gained insight into the extent to which spore and/or drift connectivity underlies the positive effect of patch connectivity identified by the GLMM.

#### 4.1. Validation methods

Parameterizing the ODE model required relating ODE model parameters to the fixed and random effects used to generate the GLMM's predictions. To do this, I focused on 2 groups of ODE parameters: fixed effect parameters, representing the GLMM's fixed effects (urchin density, patch connectivity, and patch area), and random effect parameters, whose variability could contribute to the GLMM's random effects of year and transect (Table 2). Starting with the fixed effects, urchin density was simply equivalent to

the ODE parameter u (Table 2). Connectivity was less straightforward—unlike the GLMM, the ODE model distinguishes between the input of spores ( $\varepsilon_s$ ) and drift  $(\varepsilon_d)$ . To relate observed values of patch connectivity to  $\varepsilon_s$  and  $\varepsilon_d$ , I explicitly calculated connectivity of spores and drift as a function of dispersal times and source patch biomasses. These calculations required a number of intermediary parameters whose values were uncertain (indicated in bold in Table 2). To account for the compounding effects of this uncertainty, I used an ensemble approach in which I stochastically generated values of each intermediate parameter (using available data to inform their probability distributions when possible) and calculated the resulting values of  $\varepsilon_s$  and  $\varepsilon_d$  (see Section 5 in the Supplement for more details). This produced distributions of  $\varepsilon_s$  and  $\varepsilon_d$ estimates for each value of patch connectivity, enabling me to capture a range of possible relationships between this GLMM fixed effect and levels of spore and drift connectivity in the ODE model.

To represent random effects in my ODE model, I focused on parameters that serve as proxies for kelp productivity, recruitment conditions, and disturbance regimes (Table 2), as all of these are likely to underlie observed 'random' variability in kelp dynamics across transects and years (Reed et al. 1996, Graham et al. 1997, Castorani et al. 2022a). I set random effects equal to 0 when generating GLMM predic-

tions, meaning that the outputs reflect impacts of the fixed effects on kelp state in an otherwise average transect and year (Zuur et al. 2009). To replicate these average conditions in the ODE model, I first used available data to estimate the frequencies at which different values of my random effect parameters (e.g. favorable recruitment conditions, severe storm disturbances, etc.) occurred across the transects and years in the GLMM dataset (Table S5). Then, for a given set of fixed effect parameters — urchin density (u) and the connectivity parameters  $(\varepsilon_s \text{ and } \varepsilon_d)$  (Table 2) — I repeated my ODE simulations (described below) with multiple combinations of random effect parameter values and weighted the outputs by the likelihood of each combination occurring (see Section 5 of the Supplement for more details). This resulted in a single ODE prediction representing a weighted average of predictions for different possible environmental conditions (i.e. combinations of random effect parameters) across the study region (Fig. S20). One assumption of this approach is that there is no covariation between random effect parameters; e.g. the probability of kelp plants having high biomass in a given year is independent of the probability of that patch experiencing good recruitment conditions. While this is an oversimplification, I verified that it is a reasonable assumption in the majority of observed cases (Fig. S22).

Table 2. Correspondence between the generalized linear mixed effects model (GLMM)'s fixed and random effects and parameters of the ordinary differential equation (ODE) model. For patch connectivity,  $b_{Ci}$  is the canopy biomass in source patch i,  $\lambda$  is the loss rate (default value =  $0.9~\rm d^{-1}$ ), and  $t_{ij}$  is the Regional Oceanic Modeling System dispersal time from source patch i to destination patch j.  $\lambda_{sii}$ ,  $\lambda_{dii}$ ,  $t_{sij}$ , and  $t_{dij}$  are loss rates and dispersal times for spores and drift, respectively.  $\theta_{ii}$ ,  $\omega_{si}$  and  $\omega_{di}$  are error terms representing uncertainty in source patch biomass and spore and drift self-retention, and  $\rho$  and d are spore and drift production rates, respectively. **Bold** indicates intermediary parameters whose values were drawn stochastically (Table S4 in the Supplement). Patch area was set to the mean of the log-transformed values in the data set (area<sub>lm</sub>); this was converted back to the original scale for calculations of  $\epsilon_s$  and  $\epsilon_d$ . Random effect parameters are as defined in Table 1, except  $I_{\rm storm}$  which is a binary indicator of whether a severe storm occurs during the simulation (see Table S5)

GLMM inputs Fixed effects		Corresponding ODE parameters Fixed effect parameters		
Effects	Calculation or value	Parameter	Calculation or value	
Urchin density	$\log(\operatorname{urchins} m^{-2} + 1)$	и	Urchins $\mathrm{m}^{-2}$	
Patch connectivity	$\log \left( \sum_{i} b_{C_i} (1 - \lambda)^{t_{ij}} + 1 \right)$	$\epsilon_s$ and $\epsilon_d$	$\varepsilon_s = \sum_{i} \frac{\boldsymbol{\theta_i} \boldsymbol{\omega_{si}} \boldsymbol{\rho} b_{C_i} (1 - \boldsymbol{\lambda_{si}})^{t_{s_{ij}}}}{\exp{(\operatorname{area_{lm}})}}$	
			$\varepsilon_d = \sum_{i} \frac{\boldsymbol{\theta}_i \boldsymbol{\omega}_{di} db_{C_i} (1 - \boldsymbol{\lambda}_{di})^{t_{d_{ij}}}}{\exp(\operatorname{area}_{lm})}$	
Patch area	$area_{lm}$		•	
Random effects		Random effect parameters		
Effects	Calculation or value	Parameter	Calculation or value	
Transect, year	0	$b$ , $G_0$ , $J_0$ , $r_{G}$ , $r_{J}$ , $\mu_{G}$ , $\mu_{J}$ , $I_{\mathrm{storm}}$	Estimate distributions of values across transects or years; calculate weighted average of ODE predictions for different values	

I used my parameterized ODE model to predict probabilities of observing kelp in the high state (the GLMM's response variable) as a function of the fixed effect parameters. For a given set of parameters, I first calculated the minimum initial kelp density  $A_{0\min}$ above which kelp would be in the high state (as defined for the GLMM) at the end of one year. Then, I approximated the probability that kelp would initially be above  $A_{0\min}$  — and thus in the high state 1 yr later — as the proportion of observed kelp densities greater than  $A_{0\min}$  (Fig. S21). The 1 yr cut-off was chosen to match the annual timescale of the data used to fit the GLMM. Each simulation began and ended in late summer (to match empirical surveys), with seasonality represented by an increase in background kelp mortality  $\mu_A$  during winter months to account for moderate-intensity winter storms. This process was repeated for the different fixed and random effect parameter combinations described above to generate probabilities of high kelp as a function of urchin density and patch connectivity.

Altogether, the above methods enabled me to produce results from my ODE model that were comparable to the GLMM's statistical predictions. I used this approach to confirm that the models predict similar probabilities of high kelp in low-connectivity scenarios (i.e. the 10% quantile of patch connectivity). Having thus validated the ODE's ability to reproduce local dynamics, I used it to explore the mechanistic underpinnings of the positive effect of high patch connectivity predicted by the GLMM. In particular, I was interested in whether drift kelp plays an important role in promoting the high kelp state, as suggested by my earlier ODE analyses (Figs. 2-4). To answer this question, I ran the ODE model with no connectivity ( $\varepsilon_s$  and  $\varepsilon_d = 0$ ), external spores only ( $\varepsilon_d =$ 0), external drift only ( $\varepsilon_s = 0$ ), and both spores and drift ( $\varepsilon_s$  and  $\varepsilon_d > 0$ ) for urchin densities between 0 and 50 ind. m<sup>-2</sup>. I repeated these simulations with multiple values from the distributions of  $\varepsilon_s$  and  $\varepsilon_d$  estimates corresponding to the 10 and 90% quantiles of patch connectivity, and compared the results to GLMM predictions for these same values of patch connectivity and urchin density.

#### 4.2. Validation results

When patch connectivity was low, the type of connectivity (spores, drift, or both) generally had minimal effects on ODE model results, as most values of  $\varepsilon_d$  and  $\varepsilon_s$  were negligibly small (Fig. 6a–c). The ODE's predictions were consistent with those of the GLMM, with both models predicting a steep decline in the probabil-

ity of kelp being in the high state as urchin density increased. Differences between the ODE and GLMM models became apparent when patch connectivity was high (Fig. 6d-f). Given that the 2 models produced similar results when patch connectivity was negligible, these differences were likely due to effects of ODE connectivity parameters  $\varepsilon_s$  and  $\varepsilon_d$  (whose exact values were uncertain, as reflected in the wide range of ODE predictions in Fig. 6d-f) rather than the ODE model being a poor representation of local dynamics. Recall that the GLMM represents the empirically based effect of patch connectivity on kelp state. Greater overlap between GLMM and ODE predictions indicates that the values of  $\varepsilon_s$  and  $\varepsilon_d$  are closer to the 'true' rates of external spore and drift input underlying empirical observations; thus, comparing the 2 models helps to identify the relative importance of spore and drift connectivity in driving the patch connectivity effect in the GLMM. For all but the lowest urchin densities, assuming only spore connectivity in the ODE model ( $\varepsilon_d = 0$ ) resulted in probabilities of high kelp in well-connected patches that were much lower than the GLMM's predictions (Fig. 6d). Including external drift input resulted in greater probabilities of kelp being in the high state that, in contrast to the spore-only scenario, largely overlapped with the GLMM. This overlap occurred in both the drift-only and drift and spore scenarios but was greater in the latter (Fig. 6e,f). Together, these results indicate that at intermediate to high urchin densities, spore connectivity alone is insufficient to produce the positive effect of patch connectivity suggested by the empirical data. The results also suggest that exchange of drift kelp may play a role in promoting the high kelp state (both on its own and by amplifying the effects of spores).

# 5. DISCUSSION

Many of the ocean's most productive and biodiverse ecosystems are characterized by patchily distributed habitat, with demographic connectivity among these patches playing a key role in the local and regional dynamics of resident species (Kritzer & Sale 2006, Cowen & Sponaugle 2009). The impacts of demographic connectivity on local population growth can depend on additional spatial processes (e.g. movement of other species or non-living resources) that produce variation in community and ecosystem structure across habitat patches (White 2007, Gounand et al. 2017). In this study, I applied a meta-ecosystem framework to interconnected kelp forest patches to explore the roles of multiple types of spatial connec-

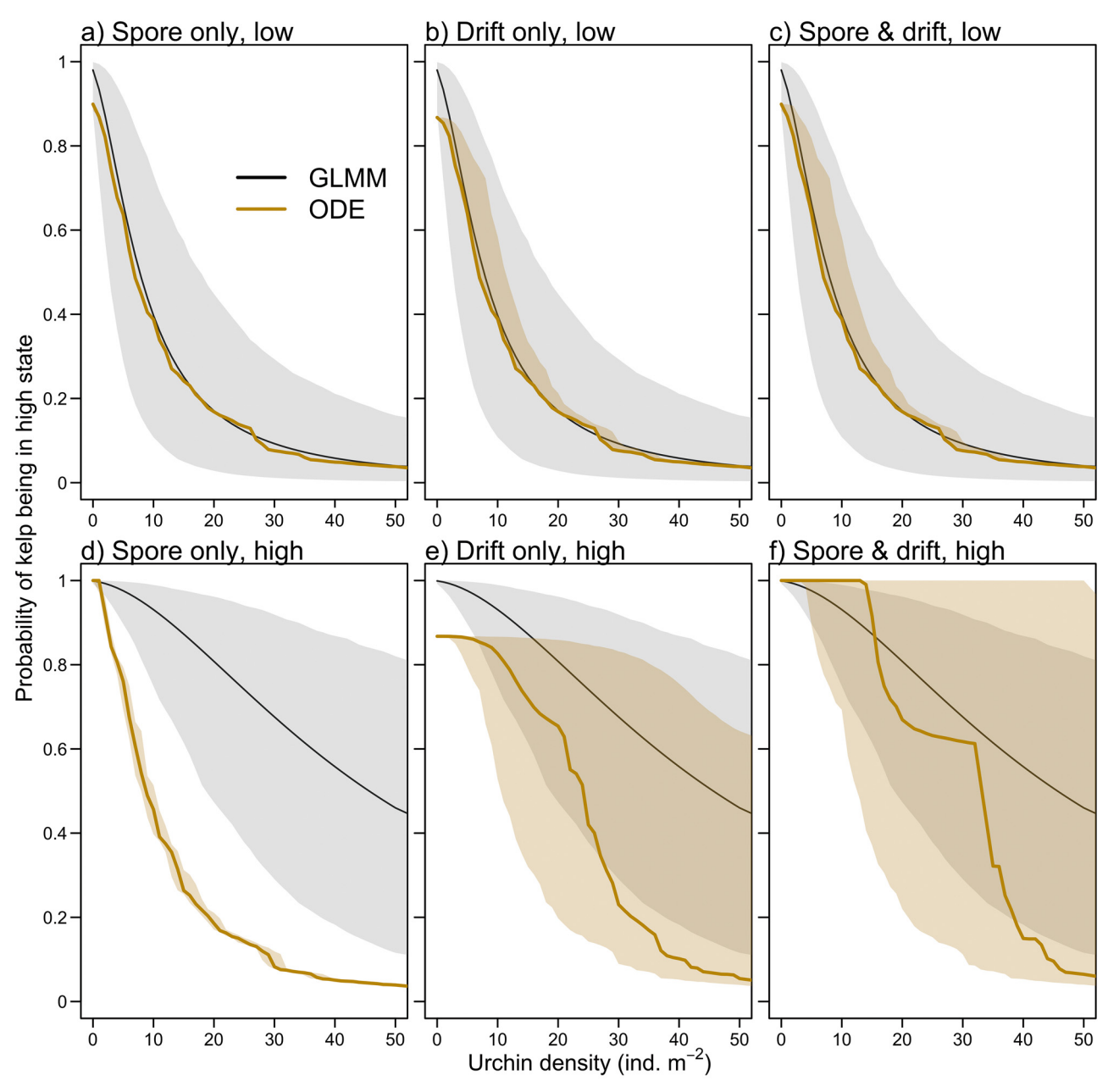


Fig. 6. Comparison of generalized linear mixed effects model (GLMM; black) and ordinary differential equation model (ODE; brown) predictions. The top and bottom rows show results for low and high connectivity scenarios (corresponding to the 10% and 90% quantiles of patch connectivity, respectively). The *x*-axis is the local density of urchins, and the *y*-axis is the probability of kelp being in the high state (> 0.05 ind. m<sup>-2</sup>). Black lines and gray shaded areas represent the mean and 95% confidence intervals of the GLMM predictions, respectively. Confidence intervals were estimated using parametric bootstrapping (n = 1000 simulations; Bolker et al. 2009). ODE predictions (brown lines) are shown for the median of simulated values of  $\varepsilon_s$  ( $\varepsilon_d$  = 0; a and d),  $\varepsilon_d$  ( $\varepsilon_s$  = 0; b and e), and both  $\varepsilon_s$  and  $\varepsilon_d$  (c and f). Brown shaded regions denote the range of ODE predictions for the central 70% (15–85% quantiles) of simulated values of  $\varepsilon_s$  (a and d),  $\varepsilon_d$  (b and e) or both  $\varepsilon_s$  and  $\varepsilon_d$  (c and f). Additional intervals are shown in Fig. S23

tivity in this system. By analyzing a mechanistic ODE model and comparing its predictions to those of a statistical model fit to empirical data, I was able to investigate how both demographic (spore) and material (drift) connectivity influence the population dynamics

of an important foundation species, giant kelp. My results suggest that the relative effects of these forms of connectivity depend on local grazing pressure, with material connectivity having a greater impact on kelp stability at higher urchin densities. This work provides

an example of how local trophic interactions and material transport can mediate metapopulation dynamics, highlighting the utility of a meta-ecosystem perspective in studies of demographically connected populations (Gounand et al. 2018).

My ODE model suggests that the connectivity of drift kelp enables kelp populations to persist at higher urchin densities and increases kelp resilience to disturbance (Figs. 2-4). These results arose from the key role of drift in mediating kelp-urchin interactions (Harrold & Reed 1985, Karatayev et al. 2021, Rennick et al. 2022): by subsidizing the food supply of urchins, external drift reduced local grazing pressure, which in turn promoted recruitment from spores (whether locally or externally produced) that may otherwise have suffered high grazing mortality. By comparing the ODE model's predictions to those of a GLMM, I was able to draw conclusions about the impacts of connectivity that were both mechanistic and grounded in empirical data. At moderate to high urchin densities, nearly all ODE predictions without drift input were outside the GLMM's confidence intervals (Fig. 6d), suggesting that external spores alone could not produce the positive effect of connectivity predicted by the GLMM at these levels of grazing. Rather, both spores and drift connectivity seem necessary, although I cannot rule out unknown processes correlated with patch connectivity that could instead contribute to its effects in the GLMM. Thus, assuming that an appreciable interpatch exchange of drift is possible (see later discussion), this work suggests that drift connectivity can be an important spatial process in kelp forest systems.

Material coupling between ecosystems of the same type (i.e. homogeneous ecosystems) has not been widely explored in meta-ecosystem literature, particularly in marine systems (Peller et al. 2021). For instance, while the fate of drift kelp has been widely studied, most of this work has been on the role of exported drift in subsidizing low-productivity beach and offshore benthic ecosystems (Vetter & Dayton 1998, Britton-Simmons et al. 2009, Hyndes et al. 2022). This focus on cross-ecosystem coupling may in part be due to the difficulty of visually distinguishing external subsidies from local production within a single ecosystem (Peller et al. 2021). As demonstrated here, applying mechanistic models to empirical systems can be a useful tool to address this challenge and may reveal that homogeneous material flows are more common than previously acknowledged. This has important implications for both metapopulations and metacommunities, as it suggests that their dynamics can be influenced by an exchange of materials (e.g. detritus,

inorganic nutrients) among component patches, as predicted by theoretical models (Marleau et al. 2010, Gravel et al. 2016). For example, using a meta-ecosystem model, Spiecker et al. (2016) showed differences in rates of material transport and organismal dispersal among local coral reefs modified the strength of local and regional trophic cascades, which in turn determined the optimal design of marine reserve networks for target species. Similarly, in this study, I found that by altering local trophic interactions, material connectivity influenced local grazing pressure and thereby mediated the potential for demographic connectivity to support local kelp populations.

An important part of the phenomenon described above is the coupled connectivity of propagules and detritus. This has the potential to occur in kelp forests for 2 reasons. First, the production of spores and drift are both proportional to kelp biomass within patches (Neushul 1963, Schiel & Foster 2015, Rennick et al. 2022). Second, both are transported by oceanographic circulation, albeit in potentially different ways depending on buoyancy and pelagic duration or degradation rates. While data for quantifying the relationship between spore and drift connectivity are currently lacking, Fig. 6 suggests a positive correlation (at least over interannual timescales), as ODE simulations in which patches received both spores and drift (Fig. 6f) were more closely aligned with empirical predictions than when spore and drift connectivity were decoupled (Fig. 6d,e). Such correlation between different forms of connectivity is unlikely to occur in all ecosystems. For example, while detrital material from terrestrial forests can be transported to adjacent ecosystems (e.g. rivers or lakes), these material flows are unlikely to follow the same patterns as the wind- or animal-driven seed dispersal connecting tree subpopulations (Gounand et al. 2018). Nevertheless, in marine systems, where currents are the primary mode of transportation for both passive propagules and non-living material, metapopulations whose patches are connected both demographically and by movement of detrital resources may be somewhat common (Spiecker et al. 2016). Whether propagules and detritus both have large impacts on ecosystem dynamics will depend on the study system, and future work should investigate the extent to which the results of the present study apply to other marine systems characterized by productive foundation species.

Another key finding of this study was that demographic (spore) connectivity alone can have limited effects on patch dynamics. This result was a consequence of a common but often overlooked feature of

meta-ecosystems: the stage-specificity of organismal dispersal and species interactions. In marine metapopulations, dispersal is often restricted to larvae or spores (Kritzer & Sale 2006, Marshall & Morgan 2011). These reproductive propagules recruit to early life stages that, in many cases, interact differently with local communities than older and larger individuals (Calado & Leal 2015). In the kelp forest system, giant kelp's dispersive spores and subsequent gametophyte and juvenile sporophyte stages must survive and mature in order for spores to contribute to populations of drift-producing adults. Early kelp life stages are vulnerable to grazing (Leonard 1994, Ng & Micheli 2022); thus, when urchins are unsatisfied by drift supply, there is a low chance of newly settled spores eventually resulting in recruitment of adult sporophytes (Dayton et al. 1984). Ignoring developmental stages in my model (i.e. assuming adults disperse) would have resulted in unrealistically strong effects of demographic connectivity, as new individuals would immediately increase local availability of drift and reduce grazing pressure. Such stage- or sizespecific interactions are prevalent in ecosystems worldwide (Miller & Rudolf 2011), yet few existing studies incorporate the stage structure of dispersing species into metacommunity or meta-ecosystem models (Gounand et al. 2018, Guzman et al. 2019). My results for the kelp forest system suggest that this omission can hinder our understanding of conditions under which demographic connectivity benefits focal populations.

Although the impacts of spore connectivity in my ODE model were generally minimal compared to drift, these predictions were dependent on recruitment parameters and local grazing pressure. Increasing rates of spore production ( $\rho$ ) and maturation of early life stages ( $r_G$  and  $r_J$ ) strengthened the effects of spore dispersal across urchin densities (Fig. S5). These parameter values resulted in unrealistically fast kelp dynamics when assumed constant; however, they could be plausible if occurring over short time intervals (Fig. S6). On natural reefs, high spore production and recruitment rates are often restricted to periods of favorable oceanographic conditions (Reed et al. 1996, 1997). In well-connected patches, the large numbers of spores received during these periods—together with their rapid development upon settlement could allow early life stages to escape grazing, resulting in observable benefits of spore connectivity on adult kelp densities (Harrold & Reed 1985). My simulations suggest that the potential for such dynamics is strongly determined by grazing pressure. At low urchin densities (less than ~5 urchins m<sup>-2</sup>), spore input

was the main driver of increased probabilities of high kelp in well-connected patches, and drift played an increasingly important role as urchin densities increased (Fig. 6d vs. 6e). Average urchin densities in each of the 25 focal kelp patches in this study were below 5 urchins m<sup>-2</sup> in 38% of annual surveys over the past 2 decades (Fig. S8) but tended to be lower in mainland than island patches (<5 urchins m<sup>-2</sup> in 57 and 26% of observations, respectively). Thus, for many of the patches examined here, and particularly those on mainland reefs, spore connectivity alone could still have a significant effect on kelp population dynamics (Castorani et al. 2015, 2017). Future work that synthesizes observations of urchin densities across a larger subset of the metapopulation would provide valuable information on the proportion of kelp patches whose dynamics are likely to be influenced by drift subsidies rather than spore connectivity alone.

By demonstrating the potential importance of drift connectivity among kelp forest patches, this study highlights the need for empirical studies that can provide more conclusive evidence than the modeling approach used here. GPS tracks of detached kelp plants along the Santa Barbara coastline (Ohlmann 2019) do demonstrate plant transport among kelp patches (Figs. S24 & S25); however, to become available to urchins, these plants would need to sink to the bottom. Alternatively, imported drift could mainly consist of fragments that already lost their buoyancy and were moved along the seafloor (Britton-Simmons et al. 2009), which would likely occur over shorter distances than surface transport. Whatever the mechanism, it is important to consider whether such drift connectivity is consistent with the high spatial heterogeneity in kelp forest systems. Adjacent urchin barren and kelp forest states are commonly observed, with drift abundance in barrens often markedly lower than in neighboring forested areas (Mattison et al. 1977, Harrold & Reed 1985, Konar & Estes 2003). Although this suggests that drift production is not exported to barren patches, low standing stocks of drift kelp in barrens could also be due to high turnover rates. Depending on local hydrodynamics and substrate characteristics, imported drift may move through without getting entrapped (possibly explaining higher barren prevalence in areas with low substrate complexity; Randell et al. 2022), and any drift that is retained is likely to be rapidly consumed by actively foraging urchins (Kriegisch et al. 2019). Indeed, several studies have found evidence of drift transport to nearby barrens (reviewed in Krumhansl & Scheibling 2012). As long as external subsidies do not satisfy urchins' energetic requirements, barren patches would still be expected

to have poorly nourished urchins and remain in a denuded state (Rennick et al. 2022). Greater empirical quantification of the magnitude and spatial scales of interpatch drift transport, as well as studies that trace the source of drift consumed by urchins within patches, will be necessary to make definitive conclusions about the role of drift connectivity in kelp forest dynamics.

The existence of neighboring barren and forested patches could indicate that the benefits of drift connectivity on kelp dynamics depend on a patch's initial state. A number of mechanisms beyond reduced drift supply can maintain urchin barrens, such as increased per capita consumption rates in barren patches (due to urchin starvation and/or lower predation risk; Dean et al. 1984, Matassa 2010, Smith et al. 2021). Thus, even if drift connectivity promotes persistence of intact kelp forests (e.g. by buffering local fluctuations in drift production), it may have limited effects once patches are in the barren state. Due to sample size limitations, I did not distinguish between kelp colonization (i.e. recovery from the low kelp state) and persistence in my statistical analyses. However, previous studies of this metapopulation found that patch connectivity had stronger effects on kelp persistence than colonization, suggesting that the magnitude of the benefits of connectivity depends on whether a patch is initially barren or forested (Castorani et al. 2015). This has important management implications, particularly in the context of kelp forest restoration (Morris et al. 2020). For example, a recent modeling study found that establishing favorable initial conditions (through urchin removal and outplanting of mature kelp) was key for the successful restoration of bull kelp on northern California reefs, as kelp spores were unable to recolonize regions where urchins were above a threshold density (Arroyo-Esquivel et al. 2023). This threshold increased with kelp outplanting intensity (Arroyo-Esquivel et al. 2023); my model suggests that drift connectivity can impact the threshold in a similar way (lower black lines in Fig. 3). However, additional barren-maintaining feedbacks not included in my model may reduce the magnitude of this connectivity effect. Future empirical and modeling studies that explore conditions under which drift transport among natural reefs promotes kelp expansion into barren regions should help inform restoration strategies.

Future studies on spatial connectivity in kelp forest systems could build upon the ODE model analyzed here by relaxing some of its assumptions about kelp and urchin dynamics. For example, due to the temporal resolution of empirical data, I ignored potential intraannual variation in most model parameters (discussed

in Section 5 of the Supplement). For simplicity, I assumed that local and externally produced drift are of comparable — and constant — nutritional value and thus contribute equally to satisfying urchins' consumptive demands. In reality, urchins may selectively feed on drift based on its state of degradation, which could impose limits on the length of time (and distance) drift can travel and still subsidize urchins in recipient patches. I also assumed that urchin densities were constant. Given urchins' long lifespans and sporadic recruitment (Okamoto et al. 2020), this was a reasonable assumption for the short (1 yr) simulations used here for comparison with empirical data. However, over longer timescales, the dependence of urchin reproduction on drift kelp (Claisse et al. 2013) could result in complex spatial interactions between kelp and urchin populations. For example, by serving as sources of urchin larvae, patches with high rates of drift production and/or import could promote barren formation in less productive or more isolated reefs (Karatayev & Baskett 2020). Urchins have a longer pelagic larval duration than kelp spores; thus, incorporating their dynamics into my model would require being explicit about spatial scales of urchin and kelp dispersal (as well as drift transport) and defining what a 'patch' represents for each species (Massol et al. 2011, Guzman et al. 2019). Such a model could then be used to explore how flows of drift kelp and urchin-kelp metacommunity dynamics influence community state across spatiotemporal scales, providing insight into longer-term consequences of patterns of drift connectivity.

# 6. CONCLUSIONS

This study shows that flows of detrital material (drift) between kelp forests may influence the extent to which demographic connectivity benefits populations of the foundation species giant kelp. These results highlight the potential for meta-ecosystem processes that couple homogeneous ecosystems to shape population and community dynamics. Here, effects of material connectivity arose due to local feedbacks in which drift subsidies reduced grazing pressure on living kelp; however, future work should explore additional ways in which material coupling may impact local interactions in both kelp forests and other ecosystems. Mechanistic models like my ODE model can be a useful tool for these types of studies, helping to disentangle the roles of empirically intractable processes and provide insight into drivers of statistical relationships. This approach is most powerful when extensive data exist for model parameterization and

validation, reinforcing the value of long-term and publicly available data sets like those used in this study.

*Data availability.* All data used in this study is published and publicly available from cited sources. Code for all analyses is available at https://doi.org/10.5281/zenodo.8317545.

Acknowledgements. I thank Holly Moeller for numerous thoughtful discussions and feedback on model development, analyses, and manuscript drafts. I also thank Daniel Reed, Cherie Briggs, and Adrian Stier for discussions and comments that greatly improved the manuscript. I thank David Kushner, Tom Bell, Max Castorani, and Li Kui for assistance with empirical data. I also thank Kyle Emery and David Siegel for helpful discussions on drift connectivity, Ferdinand Pfab for providing a code template for bifurcation analyses, and the Moeller Lab for feedback on manuscript figures. I gratefully acknowledge the work of Clint Nelson and the many students and staff of the SBC LTER and CINP KFMP programs in collecting the long-term data that made this study possible. This research was supported by a National Science Foundation (NSF) Graduate Research Fellowship to A.R.D.

#### LITERATURE CITED

- Alberto F, Raimondi PT, Reed DC, Coelho NC, Leblois R, Whitmer A, Serrão EA (2010) Habitat continuity and geographic distance predict population genetic differentiation in giant kelp. Ecology 91:49–56
- Arroyo-Esquivel J, Baskett ML, McPherson M, Hastings A (2023) How far to build it before they come? Analyzing the use of the Field of Dreams hypothesis in bull kelp restoration. Ecol Appl 33:e2850
- Bates D, Mächler M, Bolker B, Walker S (2015) Fitting linear mixed-effects models using lme4. J Stat Softw 67:1—48
- Bolker BM, Brooks ME, Clark CJ, Geange SW, Poulsen JR, Stevens MHH, White JSS (2009) Generalized linear mixed models: a practical guide for ecology and evolution. Trends Ecol Evol 24:127–135
- Britton-Simmons K, Foley G, Okamoto D (2009) Spatial subsidy in the subtidal zone: utilization of drift algae by a deep subtidal sea urchin. Aquat Biol 5:233—243
- Burgess SC, Nickols KJ, Griesemer CD, Barnett LAK and others (2014) Beyond connectivity: how empirical methods can quantify population persistence to improve marine protected-area design. Ecol Appl 24:257–270
- Byrnes JE, Reed DC, Cardinale BJ, Cavanaugh KC, Holbrook SJ, Schmitt RJ (2011) Climate-driven increases in storm frequency simplify kelp forest food webs. Glob Change Biol 17:2513—2524
  - Calado R, Leal MC (2015) Trophic ecology of benthic marine invertebrates with bi-phasic life cycles. Adv Mar Biol 71: 1–70
  - Caselle JE, Hamilton SL, Warner RR (2003) The interaction of retention, recruitment, and density-dependent mortality in the spatial placement of marine reserves. Gulf Caribb Res 14:107–117
- Castorani MCN, Reed DC, Alberto F, Bell TW and others (2015) Connectivity structures local population dynamics: a long-term empirical test in a large metapopula-

- tion system. Ecology 96:3141-3152
- Castorani MCN, Reed DC, Raimondi PT, Alberto F and others (2017) Fluctuations in population fecundity drive variation in demographic connectivity and metapopulation dynamics. Proc R Soc B 284:20162086
- Castorani MCN, Harrer SL, Miller RJ, Reed DC (2021) Disturbance structures canopy and understory productivity along an environmental gradient. Ecol Lett 24: 2192–2206
  - Castorani MCN, Bell TW, Walter JA, Reuman DC, Cavanaugh KC, Sheppard LW (2022a) Disturbance and nutrients synchronise kelp forests across scales through interacting Moran effects. Ecol Lett 25:1854—1868
- Castorani MCN, Reed DC, Raimondi PT, Alberto F, Bell TW, Cavanaugh KC, Siegel DA (2022b) Kelp metapopulations: semi-annual time series of giant kelp patch area, biomass and fecundity in southern California, 1996—2006 ver 2. Environmental Data Initiative, https://doi.org/10.6073/pasta/4c5a27154458ece5585384339eb0c2ee
- Castorani MCN, Siegel DA, Simons RD, Reed DC, Raimondi PT, Alberto F (2022c) Kelp metapopulations: semi-annual time series of spore dispersal times among giant kelp patches in southern California, 1996—2006 ver 4. Environmental Data Initiative, https://doi.org/10.6073/pasta/d1107107e7c9ebc6476dfbe9e64eb6cb
- Cavanaugh KC, Siegel DA, Raimondi PT, Alberto F (2014) Patch definition in metapopulation analysis: a graph theory approach to solve the mega-patch problem. Ecology 95:316—328
- Cavanaugh KC, Siegel DA, Raimondi PT, Alberto F (2019) SBC LTER: spatial definitions of giant kelp (*Macrocystis pyrifera*) patches in southern and central California ver 2. Environmental Data Initiative, https://doi.org/10.6073/pasta/97ef540ba3fc62dff50779533bb39466
- Claisse JT, Williams JP, Ford T, Pondella DJ, Meux B, Protopapadakis L (2013) Kelp forest habitat restoration has the potential to increase sea urchin gonad biomass. Ecosphere 4:38
- Cowen RK, Sponaugle S (2009) Larval dispersal and marine population connectivity. Annu Rev Mar Sci 1:443–466
- Dayton PK, Currie V, Gerrodette T, Keller BD, Rosenthal R, Tresca DV (1984) Patch dynamics and stability of some California kelp communities. Ecol Monogr 54: 253–289
- Dean TA, Schroeter SC, Dixon JD (1984) Effects of grazing by two species of sea urchins (Strongylocentrotus franciscanus and Lytechinus anamesus) on recruitment and survival of two species of kelp (Macrocystis pyrifera and Pterygophora californica). Mar Biol 78:301—313
- Dedrick AG, Catalano KA, Stuart MR, White JW, Montes HR, Pinsky ML (2021) Persistence of a reef fish metapopulation via network connectivity: theory and data. Ecol Lett 24:1121–1132
- Detmer AR, Miller RJ, Reed DC, Bell TW, Stier AC, Moeller HV (2021) Variation in disturbance to a foundation species structures the dynamics of a benthic reef community. Ecology 102:e03304
- Dugan JE, Hubbard DM, Page HM, Schimel JP (2011) Marine macrophyte wrack inputs and dissolved nutrients in beach sands. Estuar Coasts 34:839–850
- Gaylord B, Reed DC, Raimondi PT, Washburn L (2006)
  Macroalgal spore dispersal in coastal environments:
  mechanistic insights revealed by theory and experiment.
  Ecol Monogr 76:481–502
- Gouhier TC, Guichard F, Menge BA (2013) Designing effec-

- tive reserve networks for nonequilibrium metacommunities. Ecol Appl 23:1488–1503
- Gounand I, Harvey E, Ganesanandamoorthy P, Altermatt F (2017) Subsidies mediate interactions between communities across space. Oikos 126:972—979
- Gounand I, Harvey E, Little CJ, Altermatt F (2018) Metaecosystems 2.0: rooting the theory into the field. Trends Ecol Evol 33:36–46
- Graham MH, Harrold C, Lisin S, Light K, Watanabe JM, Foster MS (1997) Population dynamics of giant kelp *Macrocystis pyrifera* along a wave exposure gradient. Mar Ecol Prog Ser 148:269–279
- Gravel D, Mouquet N, Loreau M, Guichard F (2010) Patch dynamics, persistence, and species coexistence in metaecosystems. Am Nat 176:289—302
- Gravel D, Massol F, Leibold MA (2016) Stability and complexity in model meta-ecosystems. Nat Commun 7:12457
- Grimm V, Reise K, Strasser M (2003) Marine metapopulations: A useful concept? Helgol Mar Res 56:222–228
- Guichard F (2017) Recent advances in metacommunities and meta-ecosystem theories. F1000 Res 6:610
- Guzman LM, Germain RM, Forbes C, Straus S and others (2019) Towards a multi-trophic extension of metacommunity ecology. Ecol Lett 22:19—33
- Harrold C, Reed DC (1985) Food availability, sea urchin grazing, and kelp forest community structure. Ecology 66:1160–1169
- Hyndes GA, Berdan EL, Duarte C, Dugan JE and others (2022) The role of inputs of marine wrack and carrion in sandy-beach ecosystems: a global review. Biol Rev Camb Philos Soc 97:2127—2161
- \*Karatayev VA, Baskett ML (2020) At what spatial scales are alternative stable states relevant in highly interconnected ecosystems? Ecology 101:e02930
- \*Karatayev VA, Baskett ML, Kushner DJ, Shears NT, Caselle JE, Boettiger C (2021) Grazer behaviour can regulate large-scale patterning of community states. Ecol Lett 24: 1917–1929
  - Koen-Alonso M (2007) A process-oriented approach to the multispecies functional response. In: Rooney N, McCann KS, Noakes DLG (eds) From energetics to ecosystems: the dynamics and structure of ecological systems. Springer, Dordrecht, p 1–36
- Konar B, Estes JA (2003) The stability of boundary regions between kelp beds and deforested areas. Ecology 84: 174–185
- Kriegisch N, Reeves SE, Flukes EB, Johnson CR, Ling SD (2019) Drift-kelp suppresses foraging movement of overgrazing sea urchins. Oecologia 190:665–677
  - Kritzer JP, Sale PF (eds) (2006) Marine metapopulations. Academic Press, San Diego, CA
- Krumhansl KA, Scheibling RE (2012) Production and fate of kelp detritus. Mar Ecol Prog Ser 467:281–302
- Kushner D, Rassweiler A, McLaughlin JP, Lafferty KD (2013) A multi-decade time series of kelp forest community structure at the California Channel Islands. Ecology 94: 2655
- Leonard GH (1994) Effect of the bat star Asterina miniata (Brandt) on recruitment of the giant kelp Macrocystis pyrifera C. Agardh. J Exp Mar Biol Ecol 179:81—98
- Ling SD, Scheibling RE, Rassweiler A, Johnson CR and others (2015) Global regime shift dynamics of catastrophic sea urchin overgrazing. Proc R Soc B 370:20130269
- Loreau M, Mouquet N, Holt RD (2003) Meta-ecosystems: a theoretical framework for a spatial ecosystem ecology.

- Ecol Lett 6:673-679
- Marleau JN, Guichard F, Mallard F, Loreau M (2010) Nutrient flows between ecosystems can destabilize simple food chains. J Theor Biol 266:162–174
- Marleau JN, Guichard F, Loreau M (2014) Meta-ecosystem dynamics and functioning on finite spatial networks. Proc R Soc B 281:20132094
- Marshall DJ, Morgan SG (2011) Ecological and evolutionary consequences of linked life-history stages in the sea. Curr Biol 21:R718–R725
- Massol F, Gravel D, Mouquet N, Cadotte MW, Fukami T, Leibold MA (2011) Linking community and ecosystem dynamics through spatial ecology: an integrative approach to spatial food webs. Ecol Lett 14:313—323
- Matassa CM (2010) Purple sea urchins Strongylocentrotus purpuratus reduce grazing rates in response to risk cues from the spiny lobster Panulirus interruptus. Mar Ecol Prog Ser 400:283–288
- Mattison JE, Trent JD, Shanks AL, Akin TB, Pearse JS (1977) Movement and feeding activity of red sea urchins (*Strongylocentrotus franciscanus*) adjacent to a kelp forest. Mar Biol 39:25–30
- Miller TEX, Rudolf VHW (2011) Thinking inside the box: community-level consequences of stage-structured populations. Trends Ecol Evol 26:457–466
- Miller RJ, Lafferty KD, Lamy T, Kui L, Rassweiler A, Reed DC (2018) Giant kelp, *Macrocystis pyrifera*, increases faunal diversity through physical engineering. Proc R Soc B 285: 20172571
- Morris RL, Hale R, Strain EMA, Reeves SE and others (2020) Key principles for managing recovery of kelp forests through restoration. BioScience 70:688–698
- Neushul M (1963) Studies on the giant kelp, *Macrocystis*. II. Reproduction. Am J Bot 50:354—359
- Ng CA, Micheli F (2022) Variability in grazing on juvenile giant kelp throughout an upwelling season. Mar Ecol Prog Ser 693:83–93
  - Ohlmann C (2019) Data from freely drifting kelp plants tagged with drifters in the Santa Barbara Channel between November of 2015 and December of 2017. Biological and Chemical Oceanography Data Management Office. https://www.bco-dmo.org/dataset/739111
- Okamoto DK, Schroeter SC, Reed DC (2020) Effects of ocean climate on spatiotemporal variation in sea urchin settlement and recruitment. Limnol Oceanogr 65:2076—2091
- Peller T, Andrews S, Leroux SJ, Guichard F (2021) From marine metacommunities to meta-ecosystems: examining the nature, scale and significance of resource flows in benthic marine environments. Ecosystems 24: 1239–1252
- Polis GA, Anderson WB, Holt RD (1997) Toward an integration of landscape and food web ecology: the dynamics of spatially subsidized food webs. Annu Rev Ecol Syst 28: 289–316
  - R Core Team (2021) R: a language and environment for statistical computing. R Foundation for Statistical Computing, Vienna
- Randell Z, Kenner M, Tomoleoni J, Yee J, Novak M (2022) Kelp-forest dynamics controlled by substrate complexity. Proc Natl Acad Sci USA 119:e2103483119
- Rassweiler A, Reed DC, Harrer SL, Nelson JC (2018) Improved estimates of net primary production, growth, and standing crop of *Macrocystis pyrifera* in Southern California. Ecology 99:2132
- Reed DC (1990) The effects of variable settlement and early

- competition on patterns of kelp recruitment. Ecology 71: 776-787
- Reed DC, Ebeling AW, Anderson TW, Anghera M (1996)
  Differential reproductive responses to fluctuating resources in two seaweeds with different reproductive strategies. Ecology 77:300—316
- Reed DC, Anderson TW, Ebeling AW, Anghera M (1997)
  The role of reproductive synchrony in the colonization potential of kelp. Ecology 78:2443—2457
- Reed DC, Schroeter SC, Raimondi PT (2004) Spore supply and habitat availability as sources of recruitment limitation in the giant kelp *Macrocystis pyrifera* (Phaeophyceae) 1: colonization in giant kelp. J Phycol 40:275–284
  - Reed DC, Kinlan BP, Raimondi PT, Washburn L, Gaylord B, Drake PT (2006) A metapopulation perspective on the patch dynamics of giant kelp in southern California. In: Kritzer JP, Sale PF (eds) Marine metapopulations. Elsevier, Burlington, MA, p 353–386
- Reed DC, Rassweiler A, Carr MH, Cavanaugh KC, Malone DP, Siegel DA (2011) Wave disturbance overwhelms top-down and bottom-up control of primary production in California kelp forests. Ecology 92:2108—2116
- Rennick M, DiFiore BP, Curtis J, Reed DC, Stier AC (2022)
  Detrital supply suppresses deforestation to maintain
  healthy kelp forest ecosystems. Ecology 103:e3673
  - Sale PF, Hanski I, Kritzer JP (2006) The merging of metapopulation theory and marine ecology: establishing the historical context. In: Kritzer JP, Sale PF (eds) Marine metapopulations. Elsevier, Burlington, MA, p 3-28
- SBC LTER Reed DC, Miller RJ (2022a) SBC LTER: reef: kelp forest community dynamics: abundance and size of giant kelp (*Macrocystis pyrifera*), ongoing since 2000 ver 26. Environmental Data Initiative, https://doi.org/10.6073/pasta/7d7b640d5cafd29c00a647f6016e165d
- SBC LTER Reed DC, Miller RJ (2022b) SBC LTER: reef: kelp

Editorial responsibility: Simonetta Fraschetti, Naples, Italy Reviewed by: 2 anonymous referees

- forest community dynamics: invertebrate and algal density ver 29. Environmental Data Initiative, https://doi.org/10.6073/pasta/da35d83d200341c27ce50348e1835971
- Schiel DR, Foster MS (2015) The biology and ecology of giant kelp forests. University of California Press, Oakland, CA
- Shears NT, Kushner DJ, Katz SL, Gaines SD (2012) Reconciling conflict between the direct and indirect effects of marine reserve protection. Environ Conserv 39:225–236
- Sitters J, Atkinson CL, Guelzow N, Kelly P, Sullivan LL (2015) Spatial stoichiometry: cross-ecosystem material flows and their impact on recipient ecosystems and organisms. Oikos 124:920—930
- Smith JG, Tomoleoni J, Staedler M, Lyon S, Fujii J, Tinker MT (2021) Behavioral responses across a mosaic of ecosystem states restructure a sea otter—urchin trophic cascade. Proc Natl Acad Sci USA 118:e2012493118
  - Soetaert K, Petzoldt T, Setzer RW (2010) Solving differential equations in R: package deSolve. J Stat Softw 33:1–25
- Spiecker B, Gouhier TC, Guichard F (2016) Reciprocal feedbacks between spatial subsidies and reserve networks in coral reef meta-ecosystems. Ecol Appl 26:264—278
- Vanderklift MA, Wernberg T (2008) Detached kelps from distant sources are a food subsidy for sea urchins. Oecologia 157:327—335
- Vetter EW, Dayton PK (1998) Macrofaunal communities within and adjacent to a detritus-rich submarine canyon system. Deep Sea Res II 45:25-54
- White JW (2007) Spatially correlated recruitment of a marine predator and its prey shapes the large-scale pattern of density-dependent prey mortality. Ecol Lett 10:1054–1065
- White JW, Samhouri JF (2011) Oceanographic coupling across three trophic levels shapes source—sink dynamics in marine metacommunities. Oikos 120:1151–1164
  - Zuur AF, Ieno EN, Walker N, Saveliev AA, Smith GM (2009) Mixed effects models and extensions in ecology with R. Springer, New York, NY

Submitted: June 1, 2023 Accepted: October 25, 2023

Proofs received from author(s): January 5, 2024